Impact of scattering on secrecy outage probability of underwater optical wireless links

Rubén Boluda-Ruiz, Pedro Salcedo-Serrano, Beatriz Castillo-Vázquez, Antonio García-Zambrana, and José María Garrido-Balsells

Abstract

The analysis of physical layer security aspects in underwater optical wireless communication (UOWC) systems is attracting considerable attention in recent years due to the increasing need to transmit large and secure amounts of data. This paper, therefore, performs a careful investigation of the secrecy outage probability (SOP) of UOWC systems over Weibull oceanic turbulence channels with angular misalignment errors that are affected by absorption and scattering. The SOP performance is then evaluated under the intercepting attempt of underwater eavesdroppers or unauthorized drones that search an opportunity to capture radiated power with the goal of decreasing the channel capacity of the main channel or increasing the probability of an unsecured communication. In this way, novel approximate closed-form solutions are derived for the SOP, which are corroborated by Monte Carlo simulations in different real scenarios such as clear ocean and coastal waters that are modeled by a determined chlorophyll-a concentration. The results show that the effect of scattering plays a crucial role in determining which kind of water is more secure in terms of SOP performance for different severity of pointing errors.

Index Terms

Underwater free-space optical, physical layer security (PHY), absorption, scattering, oceanic turbulence, and misalignment errors.

I. Introduction

Underwater optical wireless communication (UOWC) systems are coming to the world's oceans. Both scientific community and industry are well aware of the important need to transmit

Rubén Boluda-Ruiz, Pedro Salcedo-Serrano, Beatriz Castillo-Vázquez, Antonio García-Zambrana, and José María Garrido-Balsells are with the Wireless Optical Communications Lab., Telecommunication Research Institute (TELMA), Universidad de Málaga, Málaga, Spain (e-mail: rbr@ic.uma.es, pss@ic-uma.es, bcv@ic.uma.es, agz@ic.uma.es, and jmgb@ic.uma.es).

large amounts of data at high speed by means of secure submarine wireless links [1]–[3]. This fact is undoubtedly driven by an intensification of activities related to ocean observation, offshore exploration and construction, environmental surveillance for the prevention of natural disasters, as well as by the search for raw materials such as oil and gas, among other key applications. Within this context, both autonomous underwater vehicles (AUV) and remotely operated vehicles (ROV), which are equipped with modern technology to monitor the sea, play a pivotal role, making this kind of activities possible [4]. Thus, due to the rapid technological development of these underwater drones and in an increasingly ocean full of such devices, it is essential to guarantee the exchange of private information between them [5], since it becomes more challenging as we extend into deeper, remote and hostile marine environments. This has not been conventionally addressed yet by considering the main degrading factors of the UOWC channel. However, this is not the case of terrestrial free-space optical (FSO) and indoor visible light communication (VLC) systems where aspects about physical layer security (PHY) in the presence of passive and active eavesdroppers have been extensively investigated in recent years [6]–[11] (and references therein). This explosion in the underwater drones market, which is expected to keep growing at a rate of 20.8% until 2025 [12], should have been accompanied by a similar discussion on privacy concerns.

Unlike traditional security approaches such as cryptographic encryption methods, physical layer security takes most advantage of the randomness of the underwater optical channel to improve the secrecy performance [13]. In this way, the proposed theory in the context of FSO and VLC systems cannot be directly applied to UOWC systems, since the underwater optical channel presents some specificities that must be analyzed carefully. But still, there is some progress in the context of mixed dual-hop radio-frequency (RF)-UOWC systems [14]–[17], where different relaying strategies such as amplify-and-forward (AF) and decode-and-forward (DF) were proposed to analyze the secrecy performance when the RF link is subject to eavesdropping due to aerial drones. At the same time, some authors have explored the limits of the achievable secrecy rate over ocean quantum links [18], as well as it was concluded in [19] that safety might be compromised as the link distance increases. More recently, the impact of surface fluctuations and scattering have been analyzed in the context of physical layer security for UOWC systems based on the water-to-air interface when using light emitting diodes (LED) [20]. As can be noticed, none of these works has considered the impact of assuming an underwater eavesdropper on the secrecy performance, which represents a practical scenario due to a greater presence

of underwater devices in our oceans. Although laser beam technology is inherently safe, the transmitted optical beam suffers from divergence owing to scattering and oceanic turbulence [21]–[26] (and references therein). In this sense, a potential eavesdropping would take place when the underwater eavesdropper is positioned within the divergence region of the laser beam. In practice, this provokes that the eavesdropper is relatively near the main receiver. Besides, the longer link distance, the greater opportunity to capture radiated power. This kind of practical scenarios has not been deeply explored in the ocean yet in the current literature. This paper, therefore, pretends to fill this gap where the scattering phenomenon, as well as the kind of water are expected to have a major impact on secrecy performance.

In this paper, we carry out a careful research of the secrecy performance of UOWC systems over Weibull oceanic turbulence channels with angular pointing errors in the presence of absorption and scattering, and under the intercepting attempt of underwater eavesdroppers or unauthorized drones. In this context, we obtain a novel approximate closed-form expression for the secrecy outage probability (SOP), which is verified by exact Monte Carlo simulations, for different kinds of water such as clear ocean and coastal waters that are modeled by different chlorophyll-a concentrations. The chlorophyll-a concentration model proposed by Haltrin in [27] is used, since it allows to express all inherent optical properties (IOP) of seawater by a single parameter. Others models such as the one proposed in [28], among other, can be also used to take into account planktonic components covering different sizes. We also develop a new asymptotic solution that will allow simple mathematical treatment to explore how key channel parameters influence on SOP performance at high signal-to-noise-ratio (SNR). As a new feature in SOP performance, we also include the effect of undersea angular misalignment errors, as proposed in [23], by modeling the additional geometric spread at the receivers due to scattering. The traditional pointing errors model is then refined to include the effect of scattering by computing the true received power at the receiver. In line with this, one of the most fascinating conclusions is that the kind of water presents a remarkably impact on secrecy performance, never seen before, where coastal water scenarios may be even more secure than clear ocean water for the same link distance, depending fundamentally on transmitter source parameters such as the beam divergence angle, and the severity of pointing errors. Monte Carlo simulations are further included to confirm the theoretical performance analysis.

The balance of this work is arranged as follows. In Section II, the system and channel models are illustrated. The SOP performance analysis is carried out in Section III, as well as some

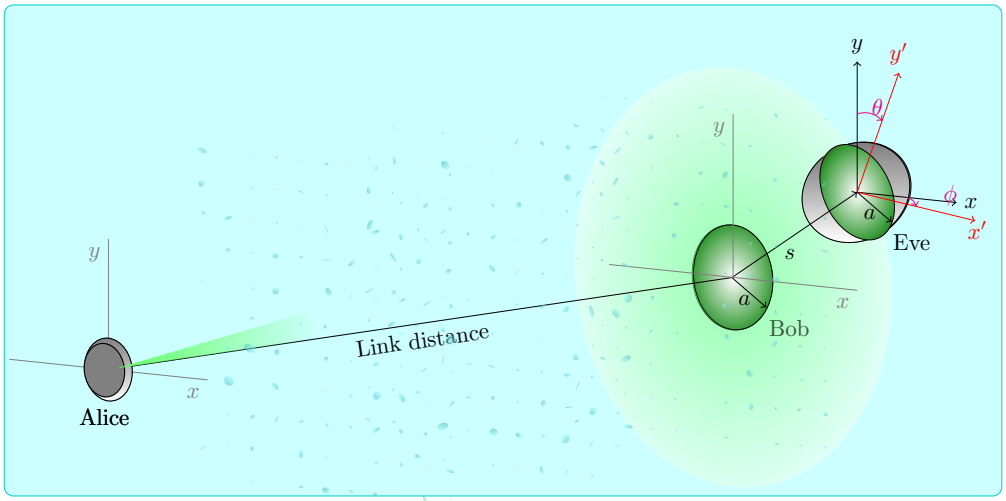

Fig. 1: Block diagram under study where the boresight error, as computed by $s = \sqrt{\mu_x^2 + \mu_y^2}$, signifies the underwater eavesdropper's position in the xy-plane, and the angles θ and ϕ stand for the rotation of the underwater eavesdropper, respectively.

numerical results and discussion on realistic UOWC scenarios are afforded in Section IV. Finally, this work is concluded in Section V.

II. System and Channel Models

A. System model

As commented in the preceding section, the classic Wyner's wiretap channel is considered to analyze physical layer security aspects for UOWC systems where two legitimate peers (Alice and Bob) desire to interchange privacy messages before the *eyes* of an underwater eavesdropper [13]. In order to model the system, we propose to use two different statistical distributions depending on whether the received optical beam is orthogonal or non-orthogonal with respect to the receiver plane, as illustrated in Fig. 1. In other words, we make a distinction between the geometric spread and pointing error models of the main and wiretap channels. Unlike terrestrial FSO systems, this approach has never been used in the open literature to study privacy concerns in maritime scenarios. As can be observed, the received optical beam at the eavesdropper's receiver is not assumed to be orthogonal with respect to the receiver plane, since a more practical and realistic scenario supposes that potential AUVs and ROVs that travel underwater may have a chance to be within the divergence area of the laser footprint at the main receiver. In an

TABLE I: Absorption (c_1), scattering (c_2), and extinction coefficient (c) values for $\lambda = 532$ nm.

Water type	α	$c_1[m^{-1}]$	$c_2[m^{-1}]$	$c[m^{-1}]$
Clear ocean	0.998	0.114	0.037	0.151
Coastal	0.970	0.179	0.219	0.398

undersea eavesdropping attempt, the received power by Eve will depend on how far Eve is from the footprint center. The radial displacement at the eavesdropper's receiver, r_E, is therefore distributed by the lognormal-Rice distribution [29], where the same jitter standard deviations, i.e. $\sigma_s = \sigma_x = \sigma_y$, and a nonzero boresight error, i.e. $s = \sqrt{\mu_x^2 + \mu_y^2}$, are assumed, while the radial displacement at the main receiver, r_B, is distributed by the Rayleigh distribution where the same jitter standard deviations, i.e. $\sigma_s = \sigma_x = \sigma_y$, and a zero boresight error, i.e. $s = 0$, are computed. A new strand of this paper is to model the position of the eavesdropper as the boresight displacement with respect to the center of the beamwidth. This assumption has not been adopted in any early paper, allowing to study physical layer security aspects much closer to real scenarios. Without limiting the generality, let us assume that the link spans of the main and the eavesdropper's channels are approximately equal, i.e., $d = d_B \simeq d_E$, being d the UOWC link span. Given that d is larger than the spacing among Bob and Eve, such an approximation is technically feasible.

In this context, the received SNR for each UOWC link can be expressed as

$$\text{SNR}(h_m) = \frac{2P_t^2 T_b}{\sigma_n^2} h_m^2 = 4\gamma_m^2 h_m^2, \tag{1}$$

where the subscript m is used to denote either Bob as $m = B$ or Eve as $m = E$, P_t is the average transmitted optical power by fulfilling eye-safety regulations [30], T_b is the bit period, σ_n^2 is the variance of an additive white Gaussian noise (AWGN) with zero mean, γ_m is the normalized optical SNR in the absence of oceanic turbulence and pointing errors, and h_m represents the composite fading UOWC channel under study that is composed of three terms as $h_m = h_a \cdot h_o \cdot h_p^m$. Next, we describe each of them.

B. Undersea optical channel model

Each of the UOWC channels are modeled as $h_m = h_a \cdot h_o \cdot h_p^m$, where h_a is a scaling factor that quantifies the oceanic attenuation due to absorption and scattering, h_o is the attenuation

due to salinity-induced oceanic turbulence, and h_p^m represents the attenuation due to geometric spread and pointing errors. The deterministic factor, h_a, is calculated from the Beer Lambert's law as

$$h_a \simeq \exp\left(-\alpha \cdot c \cdot d\right), \tag{2}$$

where α is a unitless parameter that is included to take into account the true received power due to scattering [22], d is the link span, and c is the extinction coefficient that is computed as $c = c_1 + c_2$ $[m^{-1}]$, i.e., the sum of the processes of absorption (c_1) and scattering (c_2) [31]. Some values for the extinction coefficient, c, are listed in Table I for a wavelength value of $\lambda = 532$ nm, which model two practical scenarios such as clear ocean and coastal waters that correspond with chlorophyll-a concentrations of 0.31 mg/m^3 and 0.83 mg/m^3, respectively [27].

By other hand, in order to consider a wide range of oceanic turbulence conditions, the Weibull oceanic turbulence model with parameters β_1 and β_2 is adopted here due to the fact that salinity gradient can be found in the open water and oceans of the world [32], [33]. At the same time, this statistical model fits well with the experimental data under practical channel conditions. In relation to the pointing error model, we use the general statistical model presented in [34] where the effect of the beamwidth, detector size, different jitter variances and nonzero boresight errors are considered. This statistical model was refined in [23] to include the effect of scattering, since the dispersive effect of the undersea optical channel makes the beam spreading increased, obtaining higher geometric losses. Thus, a closed-form expression for the probability density function (PDF) of the composite fading UOWC channel h_m was derived in [23, Eq. (17)] as follows

$$\begin{aligned} f_{h_m}(h) = &\frac{\varphi_m^2 h^{\varphi_m^2 - 1}}{\left(A_m h_a \beta_2\right)^{\varphi_m^2}} \\ &\times G_{1,2}^{2,0}\left[\left(\frac{h}{h_a A_m \beta_2}\right)^{\beta_1} \middle| \begin{matrix} 1 \\ 0, 1 - \frac{\varphi_m^2}{\beta_1} \end{matrix}\right], \end{aligned} \tag{3}$$

where $G_{p,q}^{m,n}[\cdot]$ is the Meijer's G-function [35, Eq. (9.301)]. Besides, the cumulative density function (CDF) can be easily obtained from the above expression as follows

$$F_{h_m}(h) = \frac{\varphi_m^2}{\beta_1} G_{2,3}^{2,1}\left[\left(\frac{h}{h_a A_m \beta_2}\right)^{\beta_1} \middle| \begin{matrix} 1, 1 + \frac{\varphi_m^2}{\beta_1} \\ \frac{\varphi_m^2}{\beta_1}, 1, 0 \end{matrix}\right]. \tag{4}$$

Firstly, the parameters φ_m^2 and A_m are related to the attenuation due to geometric spread and pointing errors, and they will be examined in the next subsection. Secondly, considering plane

wave propagation, β_1 and β_2 are statistical parameters that cannot be selected arbitrarily for UOWC applications, since both of them are physically related to the scintillation index, $\sigma_{h_o}^2$, and they are computed as

$$\begin{aligned} \beta_1 &\simeq \sigma_{h_o}^{-12/11}, \\ \beta_2 &= 1/\Gamma\left(1 + 1/\beta_1\right). \end{aligned} \tag{5}$$

The scintillation index, $\sigma_{h_o}^2$, is obtained for the link span, d by using the corresponding power spectrum of weak oceanic turbulence fluctuations and assuming isotropic and homogeneous waters with respect to salinity and temperature, $\Phi_n(\kappa)$ [36]. Such as power spectrum is given by

$$\begin{aligned} \Phi_n(\kappa) = 0.388 \times 10^{-8} \epsilon^{-1/3} \kappa^{-11/3} \left[1 + 2.35(\kappa\eta)^{2/3}\right] \\ \times \frac{\chi_T}{w^2}\left(w^2 e^{-A_T\delta} + e^{-A_S\delta} - 2we^{-A_{TS}\delta}\right), \end{aligned} \tag{6}$$

where ϵ denotes the turbulent kinetic energy dissipation rate, $\eta = 5 \times 10^{-3}$ m is the Kolmogorov microscale, χ_T is the temperature variance dissipation rate, $A_T = 1.863 \times 10^{-2}$, $A_S = 1.9 \times 10^{-4}$, $A_{TS} = 9.41 \times 10^{-3}$, $\delta = 8.248(\kappa\eta)^{4/3} + 12.978(\kappa\eta)^2$, and $w \in [-5, 0]$ is unitless parameter that measures the relative strength of temperature and salinity fluctuations [37], [38].

C. On the effect of scattering on misalignment errors

Let us start with the pointing error model of the main receiver Bob. Under the effect of scattering, a laser source with a Gaussian beam profile experiences an attenuation owing to geometric spread with misalignment error at the receiver, as in [23], as follows

$$h_p^B(r) \simeq k_1 A_B \exp\left(-2r^2/\omega_{z_{eqB}}^2\right), \tag{7}$$

where $\omega_{z_{eqB}}^2 = \omega_z^2\sqrt{\pi}\text{erf}(v_B)/2v\exp(-v_B^2)$ is the equivalent beamwidth, $A_B = [\text{erf}(v_B)]^2$ is the fraction of the collected power at $r_B = 0$, $v_B = \sqrt{a\pi}/\sqrt{2}\omega_z$, a is the receiver aperture radius, and $\omega_z \simeq k_2 \cdot \theta_0 \cdot d$ is the beamwidth at the receiver plane. It is noteworthy that both k_1 and k_2 are calculated by Monte Carlo simulation to model the over expansion in light beam propagation due to scattering [23], and θ_0 is the beam divergence angle at $1/e^2$. Without loss of generality, it is assumed that the legitimate channel is deployed with a boresight error near zero and, hence, the radial displacement at the main receiver, r_B, follows a Rayleigh distribution as

$$f_{r_B}(r) = \frac{r}{\sigma_B^2}\exp\left(-\frac{r^2}{2\sigma_B^2}\right), \tag{8}$$

where $\sigma_B = \sigma_s$ with σ_s being the pointing error displacement standard deviation (jitter) at the receiver. Hence, the corresponding PDF of the pointing error model of the main channel can be expressed as follows

$$f_{h_p^B}(h) = \frac{\varphi_B^2}{A_B^{\varphi_B^2}} h^{\varphi_B^2 - 1}, \;\; 0 \leq h \leq A_B, \tag{9}$$

where $\varphi_B = \omega_{z_{eqB}}/2\sigma_B$. Regarding the pointing error model at the eavesdropper's receiver, which is considered a key aspect in physical layer security for underwater FSO systems as commented before, the radial displacement, r_E, follows the lognormal-rice distribution [29, Eq. (4)]. Mathematically speaking, such a distribution is not tractable and, hence, we use a modified Rayleigh distribution, as presented in [34, Eq. (11)], to approximate it as

$$\begin{aligned} f_{r_E}(r) &= \frac{r}{\sigma_s^2} \exp\left(-\frac{r^2 + s^2}{2\sigma_s^2}\right) I_0\left(\frac{rs}{\sigma_s^2}\right) \\ &\simeq \frac{r}{\sigma_E^2} \exp\left(-\frac{r^2}{2\sigma_E^2}\right), \end{aligned} \tag{10}$$

where $\sigma_E^2 = \left((3/2)\sigma_s^4 s^2 + \sigma_s^6\right)^{1/3}$ [34, Eq. (9)], and $I_0(\cdot)$ is the modified Bessel function of the first kind with order zero. Note that the above approximation is completely valid for the pointing error values considered in this analysis, where the same jitter variances are assumed, obtaining a high accuracy. Hence, the corresponding PDF of the pointing error model of the eavesdropper's channel can be expressed as follows

$$f_{h_p^E}(h) \simeq \frac{\varphi_E^2}{A_E^{\varphi_E^2}} h^{\varphi_E^2 - 1}, \;\; 0 \leq h \leq A_E, \tag{11}$$

where $\varphi_E = \omega_{z_{eqE}}/2\sigma_E$, and the parameter A_E is obtained, as in [10, Eq. (8)], as

$$A_E = k_1 [\text{erf}(v_E)]^2 e^{\left(4\sigma_s\left(\sqrt{s^2+\sigma_s^2}-\sigma_s\right)-2\sigma_s^2\right)/\omega_{z_{eqE}}^2}, \tag{12}$$

where $v_E = \sqrt{\pi a^2 \cos\theta \cos\phi}/\sqrt{2}\omega_z$, and $\omega_{z_{eqE}}^2 = \omega_z^2\sqrt{\pi}\text{erf}(v_E)/2v_E \exp(-v_E^2)$ is the equivalent beamwidth. Finally, the parameters k_1 and k_2 that model the geometric loss in the presence of scattering are summarized in Table II for different kinds of water when a green LD with a nominal transmitted divergence angle, θ_0, of 12 mrad, a wavelength of 532 nm, and a photodetector aperture diameter of $D = 10$ cm are used, as commercial values available in [39], [40].

D. Asymptotic behavior

In the preceding subsection, we obtained the corresponding PDFs of h_m. Attention is now turned to a specific approximation to the composite fading channel, i.e., an asymptotic approximation that will allow simple mathematical manipulations to get fruitful results and discussion on

TABLE II: Geometric loss parameters for different links distances and transmit divergence angles.

Divergence angle	Clear ocean water			Coastal water		
θ_0 (mrad)	d (m)	k_1	k_2	d (m)	k_1	k_2
12	30	1.19	1	20	2.26	1.33
	35	1.22	1	25	3.02	1.42
	40	1.25	1	30	4.38	1.52

SOP performance at high SNR. Thus, the PDF of h_m is approximated as $f_{h_m}(h) \doteq a_m h^{b_m-1}$ [34], [41], using the corresponding series expansion of the Meijer's G-function [42, Eq. (07.34.06.0006.01)] as follows

$$\begin{aligned} f_{h_m}(h) &\doteq a_m h^{b_m-1} \\ &= \begin{cases} \frac{\varphi_m^2 \beta_1}{(A_m h_a \beta_2)^{\beta_1}(\varphi_m^2-\beta_1)} h^{\beta_1-1}, & \varphi_m^2 > \beta_1, \\ \frac{\varphi_m^2 \Gamma\left(1-\frac{\varphi_m^2}{\beta_1}\right)}{(A_m h_a \beta_2)^{\varphi_m^2}} h^{\varphi_m^2-1}, & \varphi_m^2 < \beta_1. \end{cases} \end{aligned} \tag{13}$$

From the above expression, it can be deduced that the asymptotic behavior of the CDF of h_m is obtained as $F_{h_m}(h) \doteq (a_m/b_m)h^{b_m}$.

III. Analysis of secrecy outage probability

In the following section, the probability of secrecy outage for UOWC systems, which is interpreted as the probability that the maximum secrecy capacity, C_s, is below a given expected secrecy rate, R_s, is thoroughly analyzed. The maximum secrecy capacity, C_s, is calculated as $C_s = [C_B - C_E]^+$ [43], where $[x]^+ = \max(x, 0)$, and $C_m = (1/2)\log_2(1 + 4\gamma_m^2 h_m^2)$ is the instantaneous capacity of each undersea optical channel, which is based on IM/DD technology and, hence, it represents a lower bound [44]. Thus, the SOP as a function of R_s is given by

$$P_{\text{out}}(R_s) := \Pr\left[C_s < R_s\right]. \tag{14}$$

Note that when $R_s < C_s$, the probability of a secure communication among Alice and Bob is not compromised at all. At this point, we can derive the SOP from the definition of C_s as

$$\begin{aligned} P_{\text{out}}(R_s) &:= \Pr\left[\log_2\left(\frac{1+4\gamma_B^2 h_B^2}{1+4\gamma_E^2 h_E^2}\right) < R_s\right] \\ &= \int_0^\infty F_{h_B}\left(\sqrt{\frac{2^{2R_s}(1+4\gamma_E^2 h^2)-1}{4\gamma_B^2}}\right) f_{h_E}(h) dh. \end{aligned} \tag{15}$$

As far as we know, it is not possible to express the above integral in closed-form, so that we need to resort to certain approximations such a lower bound (LB) and an asymptotic expression, which will be confirmed by Monte Carlo results. A lower bound for SOP is then obtained as

$$P_{\text{out}}^{\text{LB}}(R_s) \simeq \int_0^{\infty} F_{h_B}\left(2^{R_s}\frac{\gamma_E}{\gamma_B}h\right) f_{h_E}(h)dh. \tag{16}$$

Now, with the aid of [45, Eq. (2.24.1.1)] and previously substituting (3) and (4) into (16), the above integral is then expressed in a compact way as a Meijer's G-function as follows

$$\begin{aligned} P_{\text{out}}^{\text{LB}}(R_s) \simeq{}& \frac{\varphi_B^2\varphi_E^2}{\beta_1}\left(\frac{\gamma_B A_B}{2^{R_s}\gamma_E A_E}\right)^{\varphi_E^2} \\ &\times G_{4,4}^{3,2}\left[\frac{\gamma_B A_B}{2^{R_s}\gamma_E A_E}\middle| \begin{matrix} 1-\frac{\varphi_B^2}{\beta_1}-\frac{\varphi_E^2}{\beta_1}, -\frac{\varphi_E^2}{\beta_1}, 1-\frac{\varphi_E^2}{\beta_1}, 1 \\ 0, 1-\frac{\varphi_E^2}{\beta_1}, -\frac{\varphi_E^2}{\beta_1}, -\frac{\varphi_B^2}{\beta_1}-\frac{\varphi_E^2}{\beta_1} \end{matrix}\right]. \end{aligned} \tag{17}$$

A. Asymptotic secrecy outage probability analysis

As we mention earlier, a useful asymptotic expression at high SNR for the SOP can be derived by substituting (13) into (15), yielding the below integral

$$\begin{aligned} P_{\text{out}}(R_s) \doteq{}& \frac{a_B 2^{R_s b_B}}{b_B}\left(\frac{\gamma_E}{\gamma_B}\right)^{b_B} \\ &\times \int_0^{\infty}\left(h^2+\frac{1-2^{-2R_s}}{4\gamma_E^2}\right)^{\frac{b_B}{2}} f_{h_E}(h)dh. \end{aligned} \tag{18}$$

By making the following variable change $t = h^2$ and using [45, Eq. (2.24.2.4)], we can then express the above integral in a compact way as an H-Fox function, $H_{p,q}^{m,n}[\cdot]$, [46, Eq. (1.1)] as follows

$$\begin{aligned} P_{\text{out}}(R_s) &\doteq (S_c\cdot\gamma_B)^{-S_d} \\ &= \frac{a_B}{b_B\Gamma(-b_B/2)}\frac{2^{R_s b_b-1}\varphi_E^2}{(A_E h_a\beta_2)^{\varphi_E^2}}\left(\frac{1-2^{-2R_s}}{4\gamma_E^2}\right)^{\frac{b_b+\varphi_E^2}{2}} \\ &\times H_{2,3}^{3,1}\left[\left(\frac{\left(1-2^{-2R_s}\right)^{1/2}}{2\gamma_E A_E h_a\beta_2}\right)^{\beta_1}\middle| \begin{matrix}\chi_1 \\ \chi_2\end{matrix}\right]\times\gamma_B^{-b_B}. \end{aligned} \tag{19}$$

where $\chi_1 = \left\{\left(1-\frac{\varphi_E^2}{2},\frac{\beta_1}{2}\right),(1,1)\right\}$ and $\chi_2 = \left\{(0,1),\left(1-\frac{\varphi_E^2}{\beta_1},1\right),\left(\frac{-\varphi_E^2-b_B}{2},\frac{\beta_1}{2}\right)\right\}$. As can be observed from (19), the SOP can be expressed in a nice compact way as $P_{\text{out}}(R_s) \doteq (S_c\cdot\gamma_B)^{-S_d}$, where S_c and S_d stand for the secrecy gain and the secrecy diversity order, respectively. In other words, when the PDF of the combined effect of oceanic turbulence and misalignment errors

TABLE III: UOWC system setup.

Parameter	Symbol	Value
Wavelength	λ	532 nm
Responsivity	R	1 Amps per Watt
LD divergence angle at $1/e^2$	θ_0	12 mrad
Photodetector diameter	$D = 2a$	10 cm
Receiver field-of-view	FOV	180°
Link distance	d	$\{25, 30, 35, 40\}$ m
Relative strength of turbulence	w	-1
Turbulent kinetic energy dissipation rate	ϵ	$3 \times 10^{-5}\ m^2/s^3$
Temperature variance dissipation rate	χ_T	$10^{-7}\ K^2/s$
Normalized standard deviation	σ_s/a	$\{1, 2, 3, 4, 6\}$
Eavesdropper's position	$(\mu_x/a, \mu_y/a)$	$\{(3, 1), (4, 2)\}$
Eavesdropper's rotation	ρ/a	$\{0.4, 0.8\}$
Expected secrecy rate	R_s	0.5 bits/channel use

can be expanded in a Maclaurin series, the SOP can be expressed as a power series, being the first term of this series is the dominant term, i.e., $P_{\text{out}}(R_s) \doteq (S_c \cdot \gamma_B)^{-S_d}$. More interestingly, $S_d = \min(\beta_1, \varphi_B^2)$ is only dependent on communication channel between the legitimate peers Alice and Bob, while S_c depends on both channels, particularly on the communication channel between Alice and Eve.

In order to establish a reference baseline, the results with no underwater eavesdropper will be also illustrated in the next section, whose asymptotic solution at high SNR was obtained in

[47, Eq. (7)], but adopting the notation assumed in this work as

$$P_{\text{out}}^{\text{no Eve}}(R_s) \doteq (O_c \cdot \gamma_B)^{-O_d} = \left[\left(\frac{a_B (2^{R_s}-1)^{b_B/2}}{b_B 2^{b_B}} \right)^{-1/b_B} \cdot \gamma_B \right]^{-b_B}, \tag{20}$$

where O_c and O_d denote the coding gain and the outage diversity, respectively.

Finally, in order to fully grasp which the real impact of an attempt of eavesdropping on a UOWC link is, the optical SNR gap between the outage performance with no eavesdropper and the SOP performance with eavesdropper is quantified as $L[dB] \triangleq 10\log_{10}[O_c/S_c]$ after doing some easy algebraic manipulations in (19) and (20), yielding

$$\begin{aligned} L[dB] \triangleq 10\log_{10}\left[\frac{O_c}{S_c}\right] &= \frac{10}{b_B} \\ &\times \log_{10}\left[\frac{\left(2^{2R_s}-1\right)^{-b_B/2}\left(1-2^{-2R_s}\right)^{(b_B+\varphi_E^2)/2}}{2^{-b_B R_s+\varphi_E^2+1}\varphi_E^{-2}\left(A_E h_a \gamma_E \beta_2\right)^{\varphi_E^2}\Gamma\left(\frac{-b_B}{2}\right)} \right] \\ &+ \frac{10}{b_B}\log_{10}\left[H_{2,3}^{3,1}\left[\left(\frac{\left(1-2^{-2R_s}\right)^{1/2}}{2\gamma_E A_E h_a \beta_2} \right)^{\beta_1} \middle| \begin{matrix} \chi_1 \\ \chi_2 \end{matrix} \right] \right]. \end{aligned} \tag{21}$$

IV. Numerical examples and discussion

In this section, we present some numerical examples for the SOP performance under different maritime scenarios such as clear ocean and coastal waters which model different chlorophyll-a concentrations, resulting in different scattering severity, as well as under the intercepting attempt of an underwater eavesdropper with different position and rotation. For ease of reading, the UOWC system setup is summarized in Table III.

In general terms, the SOP performance is illustrated for clear ocean and coastal waters in Figs. 2, 3, 4 and 5 when different UOWC link spans, different severity of pointing errors, as well as different SNR for the eavesdropper channel, i.e. γ_E, are considered. In these figures, the lower bound on SOP, as obtained in (17), and the corresponding asymptotic closed-form expression, as obtained in (19), are both plotted as a function of the SNR of the main channel, i.e. γ_B, for an underwater eavesdropper's position of $(\mu_x/a, \mu_y/a) = (3, 1)$, as well as for an underwater eavesdropper's rotation of $\rho/a = 0.8$ with the goal of analyzing how these key parameters impact on performance in terms of security under different kind of waters. Besides, both the lower bound and the asymptotic solution present a good match with exact Monte Carlo simulations under different severity of pointing errors of $\sigma_s/a = \{1, 2, 3, 4, 6\}$. Regarding the SOP performance,

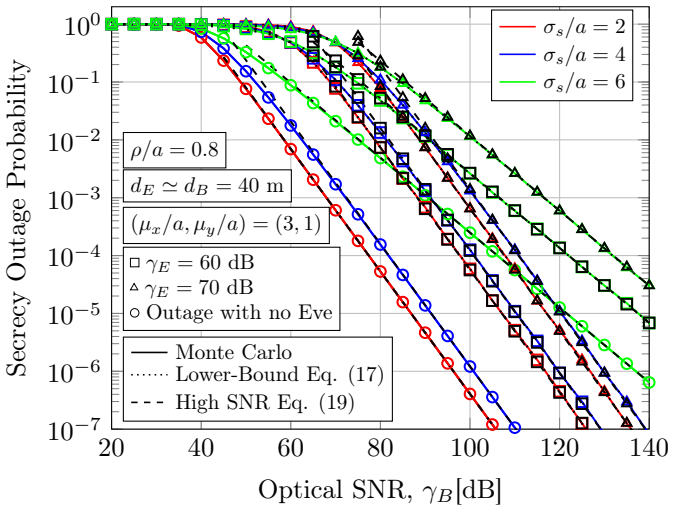

(a) Clear ocean water: $d = 35$ m and $\sigma_{h_o}^2 = 0.6$

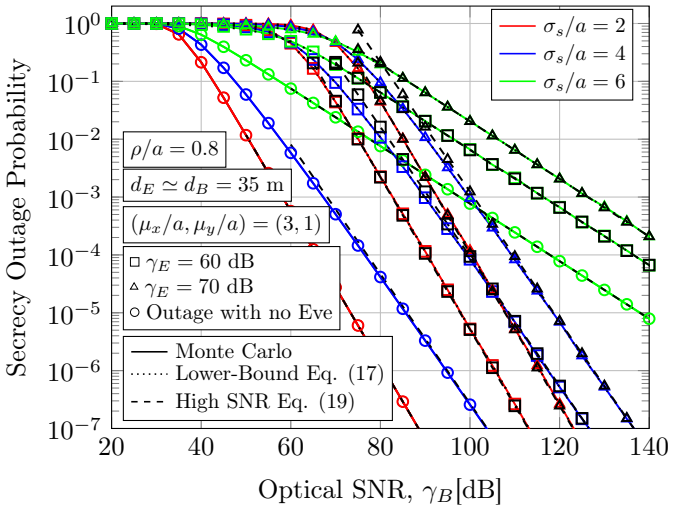

(b) Clear ocean water: $d = 40$ m and $\sigma_{h_o}^2 = 0.8$

Fig. 2: SOP performance for UOWC link distances of (a) $d = 35$ m, and (b) $d = 40$ m in clear ocean water over salinity-induced oceanic turbulence as a function of the optical SNR of the legitimate channel when an expected secrecy rate of $R_s = 0.5$ bits/channel use and a beam divergence angle of $\theta_0 = 12$ mrad are assumed.

all SOP curves have the same secrecy diversity order, i.e. $S_d = b_B$, but obtaining different shifts or SNR gap owing to the remaining UOWC system parameters. The influence of the underwater eavesdropper on the UOWC secure transmission is only reflected on the secrecy gain, S_c, which will be analyzed at the end of this section.

In Figs. 2 and 3, the SOP performance is depicted for UOWC link spans of 35 and 40 m in

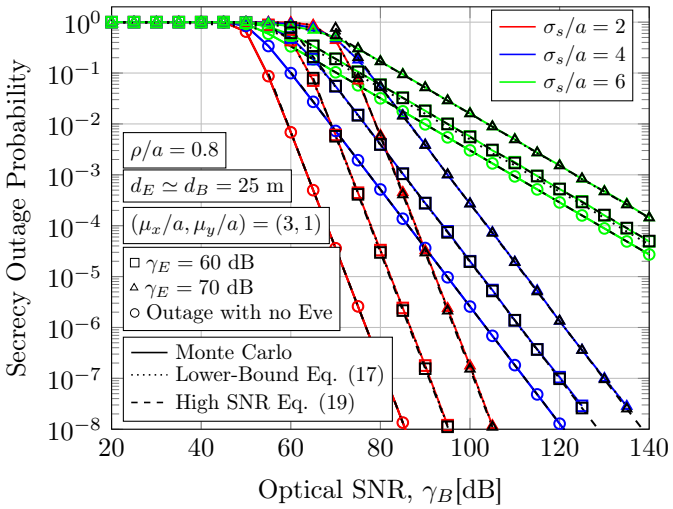

(a) Coastal water: $d = 25$ m and $\sigma_{h_o}^2 = 0.3$

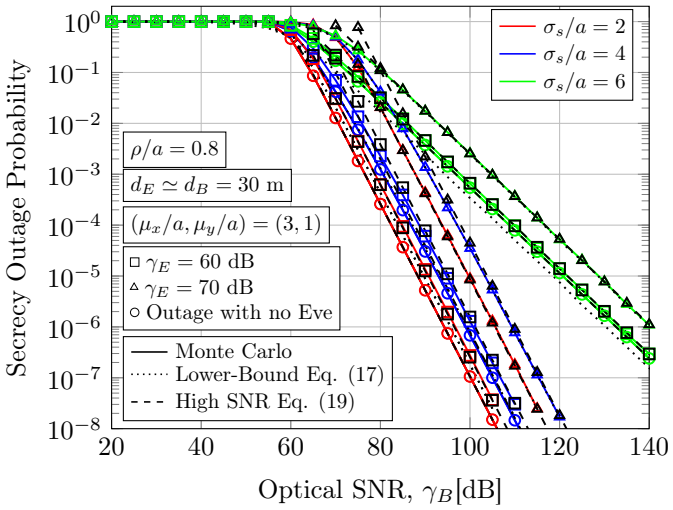

(b) Coastal water: $d = 30$ m and $\sigma_{h_o}^2 = 0.4$

Fig. 3: SOP performance for UOWC link distances of (a) $d = 25$ m, and (b) $d = 30$ m in coastal water over salinity-induced oceanic turbulence as a function of the optical SNR of the legitimate channel when an expected secrecy rate of $R_s = 0.5$ bits/channel use and a beam divergence angle of $\theta_0 = 12$ mrad are assumed.

clear ocean water, and for UOWC link spans of 25 and 30 m in coastal water. Note that the effect of jitter due mainly to ocean currents plays a key role in SOP performance, making the UOWC system be more or less secure against potential underwater eavesdropping. On the one hand, when the effect of oceanic turbulence is dominant, i.e. for jitter values of $\sigma_s/a = (2, 4)$

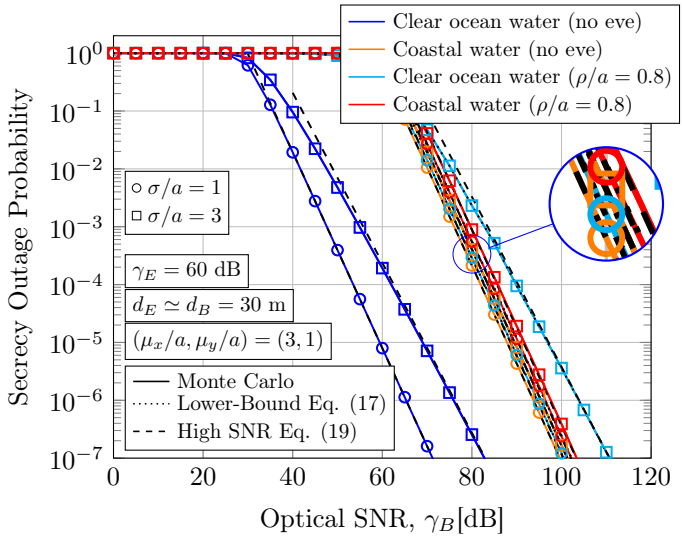

Fig. 4: SOP performance comparison between clear ocean and coastal waters for a nominal UOWC link distance of $d = 30$ m over salinity-induced oceanic turbulence as a function of the optical SNR of the legitimate channel when an expected secrecy rate of $R_s = 0.5$ bits/channel use and a beam divergence angle of $\theta_0 = 12$ mrad are assumed.

and particularly at moderate and long link distance in both types of water, the slopes of both outage capacity with no eavesdropper and the SOP performance curves are all determined by the effect of oceanic turbulence. Under this scenario, the SOP performance is strongly dependent on the quality of eavesdropper's channel, since the amount of received power by the underwater eavesdropper notably increases, as can be seen for γ_E values of 60 and 70 dB. On the other hand, when the severity of pointing errors increases, i.e., when pointing errors is dominant, the performance for a jitter value of $\sigma_s/a = 6$, the results worse considerably, and there is no difference between outage capacity with no eavesdropper and the SOP performance. In such a scenario, the slope of the SOP curve is determined by the misalignment errors.

More interestingly, the results presented in Fig. 4 become more valuable from a practical viewpoint where the SOP performance is compared for a UOWC link distance of 30 m in both clear ocean and coastal waters for an eavesdropper's position of $(\mu_x/a, \mu_y/a) = (3, 1)$. Note that a link distance of 30 m is considered convenient for the marine applications mentioned in the Introduction section in both types of water. In such a figure, we can analyze what kind of water may be more suitable in terms of physical layer security under the potential intercepting attempt of an underwater eavesdropper that can compromise the communication between the peers. On

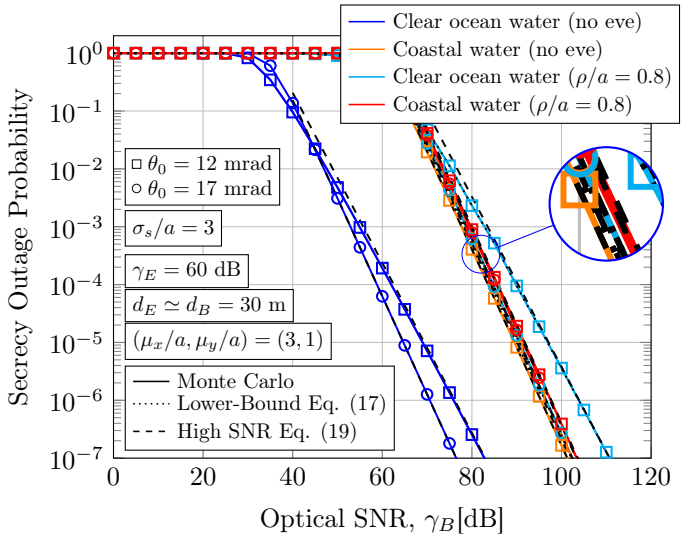

Fig. 5: SOP performance comparison between clear ocean and coastal waters for a nominal UOWC link distance of $d = 30$ m over salinity-induced oceanic turbulence as a function of the optical SNR of the legitimate channel when an expected secrecy rate of $R_s = 0.5$ bits/channel use and different transmit divergence angles of $\theta_0 = \{12, 17\}$ mrad are assumed.

the one hand, we can see that when the jitter effect takes a value of $\sigma_s/a = 1$, both clear ocean and coastal waters offer approximately the same SOP performance. Both SOP curves are separated one from the other by just a few decibels. This outcome can be contrary to the logical thinking that a maritime environment, where the effect of scattering is not significant, might offer better performance than a more turbid maritime environment in terms of physical layer security. In other words, even though clear ocean water presents a lower chlorophyll-a concentration than coastal water, both kinds of water present almost the same SOP performance where the slope of the curves is dominated by oceanic turbulence. However, the SOP performance is even worse in clear ocean water than in coastal water since a loss of almost 30 dB is obtained in comparison with the same scenario with no eavesdropper. While in coastal water, just a loss of almost 5 dB is obtained in comparison with the same scenario with no eavesdropper. It can be said that, under this scenario and considering the results plotted in this figure, a coastal water environment offers more safety to communication than a clear ocean water environment, at least when the pointing errors are not very aggressive.

On the other hand, when the effect of jitter takes a value of $\sigma_s/a = 3$, i.e., the severity of pointing errors becomes severe, the results show a very different situation. In this case, the

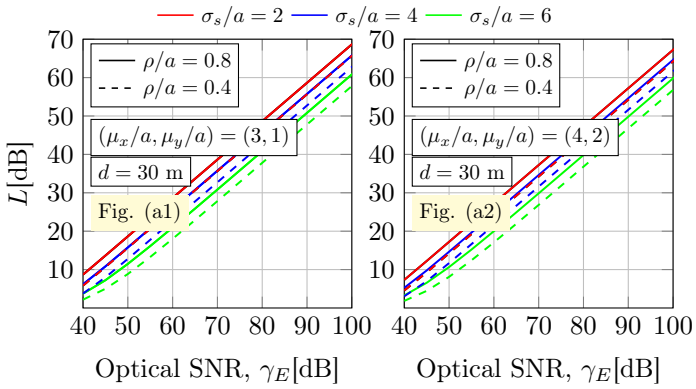

(a) Clear ocean water: $d = 30$ m and $\sigma^2_{h_o} = 0.4$

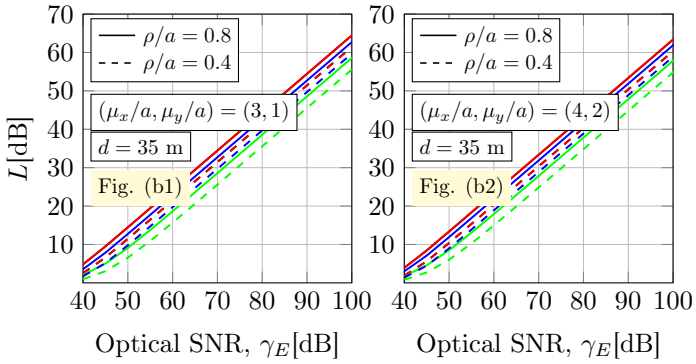

(b) Clear ocean water: $d = 35$ m and $\sigma^2_{h_o} = 0.6$

Fig. 6: Loss, L[dB], for UOWC link distances of (a) $d = 30$ m, and (b) $d = 35$ m as a function of the optical SNR, γ_E, under different severity of pointing errors, and when an expected secrecy rate of $R_s = 0.5$ bits/channel use and a beam divergence angle of $\theta_0 = 12$ mrad are assumed.

SOP performance in coastal water is superior to the SOP performance in clear ocean water, where a notable change in the slope of the SOP curves is observed, i.e., in the secrecy diversity order. In this scenario, the secrecy diversity order in clear ocean water, S_d, is dominated by the pointing errors, while in coastal water is still dominated by oceanic turbulence. For that reason, the SOP curves in clear ocean water present a smaller slope than in coastal water. The secrecy diversity depends on either oceanic turbulence or pointing errors for each kind of water due to scattering, i.e., the main degrading factor in UOWC systems, which is usually ignored or not adequately modeled by the research community. As concluded in [23], the effect of scattering on underwater light propagation produces an additional expansion of the beamwidth. This means that the geometric losses generated at the receiver plane are not the same when considering the

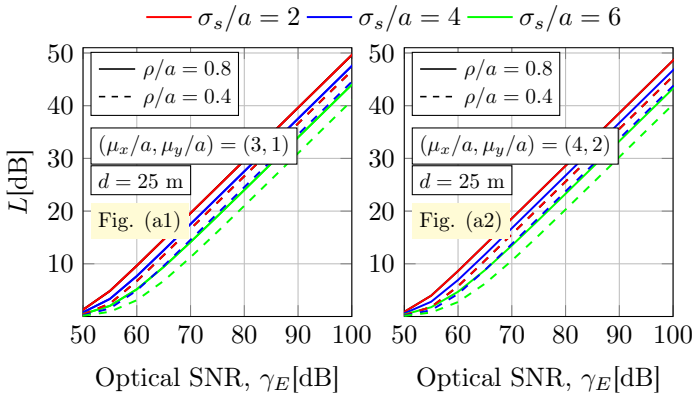

(a) Coastal water: $d = 25$ m and $\sigma^2_{h_o} = 0.3$

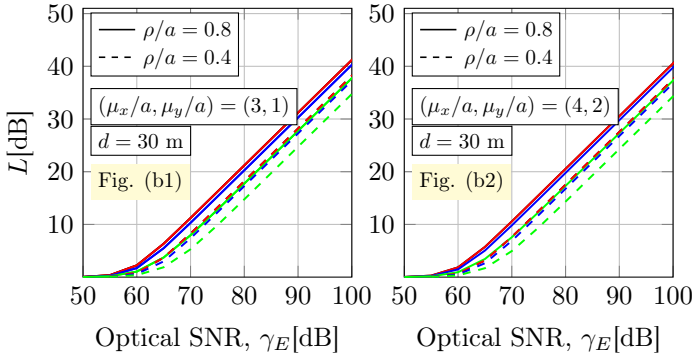

(b) Coastal water: $d = 30$ m and $\sigma^2_{h_o} = 0.4$

Fig. 7: Loss, L[dB], for UOWC link distances of (a) $d = 25$ m, and (b) $d = 30$ m as a function of the optical SNR, γ_E, under different severity of pointing errors, and when an expected secrecy rate of $R_s = 0.5$ bits/channel use and a beam divergence angle of $\theta_0 = 12$ mrad are assumed.

same link distance of 30 m in underwater scenarios such as clear ocean and coastal waters. In this way, the path loss model by (2) and the geometric spread and pointing error model by (7) proposed here for an LD source take into account the true received power at the receivers, i.e., both compute the actual received photons, even those scattered along the propagation path. The current literature usually does not consider the effect of scattering in this way [23], [48]. Therefore, this causes a greater beamwidth at the receiver plane in coastal water than in clear ocean water. This expansion, a priori, causes a more significant geometric loss. However, it also provides a natural mechanism to alleviate the jitter effect, resulting in a safer type of water from the point of view of physical layer security.

This scenario leads us to think of that perhaps the use of narrow LD sources with transmit

divergence angles below approximately 12 mrad in undersea scenarios with a low chlorophyll-a concentration such as clear ocean water is not fully suitable due to the fact that the scattering effect is not so predominant as in coastal water. For that reason, the beam footprint at the receiver plane is not large enough to mitigate the impact of jitter severity and, hence, a potential eavesdropper presents a greater opportunity to capture more effective radiated power. UOWC links based on LD sources may demand the use of larger transmit divergence angles to be able to mitigate the effect of jitter, as well as to reduce the amount of effective radiated power by the eavesdropper. For instance, one can make the beam divergence angle, θ_0, increased by reversing the orientation of an LD beam expander in order to enhance the SOP performance for short and moderate UOWC links distances [48], [49]. This is precisely what is represented in Fig. 5, i.e., the same scenario as in Fig. 4, but assuming a beam divergence angle of $\theta_0 = 17$ mrad. Note that this beam divergence angle results in being the optimum value for the scenario analyzed in Fig. 4 for clear ocean water, which was obtained through numerical optimization techniques in Mathematica (version 12.3.1.0) and subject to constraints such as $\omega_z/a > \{\sigma_x/a, \sigma_y/a\}$. Analogously, the optimum beam divergence angle for coastal water results in a value near 12 mrad, particularly, a value of 12.8 mrad for the considered scenario. As can be seen, an improvement in the secrecy diversity order, S_d, in clear ocean water can be observed, which means that for a jitter value of $\sigma_s/a = 3$, the SOP is now dominated by oceanic turbulence and, hence, the effective power captured by the eavesdropper is reduced due to the change of trend in the curves.

It is concluded that the beamwidth at the receiver plane is smaller in clear ocean water than in coastal water for the same considered distance due to the scattering effect. This phenomenon allows the underwater eavesdropper to capture more effective power under severe pointing errors, worsening the SOP performance. While in coastal water, the fact of having a larger beamwidth means that, although the underwater eavesdropper may have a greater opportunity to capture more power, this one is not as effective as in clear ocean water, as it is distributed in a Gaussian way throughout the footprint. Therefore, in absolute terms, the underwater eavesdropper collects less power in coastal water than in clear ocean water under severe pointing errors.

Finally, L[dB] is plotted as a function of γ_E for different eavesdropper's positions of $(\mu_x/a, \mu_y/a) = \{(3,1),(4$ different eavesdropper's rotation values of $\rho/a = \{0.4, 0.8\}$, and different jitter values of $\sigma_s/a = \{2, 4, 6\}$ in Figs. 6 and 7. These figures corroborate in some way the behavior observed in the previous discussion. It can be seen, firstly, how the SNR gap in dB increases drastically as the quality of the underwater eavesdropper link improves for different severity of pointing errors. Secondly,

the impact of the underwater eavesdropper's rotation is also observed. When ρ/a takes values close to 1, the underwater eavesdropper's ability to capture radiated power is maximum.

V. Conclusion

In this work, an exhaustive analysis of the SOP performance has been carried out for UOWC systems in the presence of the main degrading factors such as absorption, scattering, salinity-induced oceanic turbulence and pointing errors. New closed-form solutions have been derived for the SOP under the intercepting attempt of an underwater eavesdropper with different position and rotation. Exact Monte Carlo simulations are further included to verify the obtained bounds for different severity of scattering and oceanic turbulence.

In light of the results presented here, it can be concluded, firstly, that the kind of water and, therefore, the scattering effect, plays a crucial role when analyzing physical layer security aspects of UOWC systems in the real context of ocean observation activities. On the one hand, it cannot be affirmed that the SOP performance improves as the kind of water is purer. In other words, the SOP performance is still far from getting worse as the water becomes more turbid. The conclusions that can be drawn from this analysis are somewhat much more complex than this type of statements. Everything fundamentally revolves around the effect of scattering, i.e., the main degrading effect in this type of communication systems, much stronger than the turbulent effect of the seawater. Scattering is the phenomenon that conditions the increase or decrease of the probability of a secure communication. This probability depends on how large the beamwidth at the receiver plane is and how severe the effect of jitter is, among other things. On the other hand, it can be stated that as Eve moves away from the center of the beamwidth, the SOP performance obviously gets worse drastically. At the same time, the SOP performance improves remarkably as the link quality in terms of the optical SNR increases.

Finally, the SOP performance of UOWC systems may be improved by using multiple-input/multiple-output (MIMO) techniques that allow to considerably increase the transmitted optical power in order to reduce the combined effect of scattering and oceanic turbulence. This paper, therefore, opens a novel framework to pave the way of the analysis of physical layer security aspects that were reported from an information theory point of view with a strong focus on the kind of water, i.e., on the level of turbidity of the water.

ACKNOWLEDGMENTS

The authors are grateful for the financial support given by the Spanish MICINN Project PID2019-107792GB-I00, and the Plan Andaluz de Investigación, Desarrollo e Innovación (PAIDI) 2021 project P21_00390.

REFERENCES

[1] Z. Zeng, S. Fu, H. Zhang, Y. Dong, and J. Cheng, "A survey of underwater optical wireless communications," *IEEE Commun. Surv. & Tutorials*, vol. 19, no. 1, pp. 204–238, 2017.

[2] N. Saeed, A. Celik, T. Y. Al-Naffouri, and M.-S. Alouini, "Underwater optical wireless communications, networking, and localization: A survey," *Ad Hoc Networks*, vol. 94, p. 101935, 2019.

[3] X. Sun, C. H. Kang, M. Kong, O. Alkhazragi, Y. Guo, M. Ouhssain, Y. Weng, B. H. Jones, T. K. Ng, and B. S. Ooi, "A review on practical considerations and solutions in underwater wireless optical communication," *J. Lightwave Technol.*, vol. 38, no. 2, pp. 421–431, 2020.

[4] P. A. Hoeher, J. Sticklus, and A. Harlakin, "Underwater optical wireless communications in swarm robotics: A tutorial," *IEEE Commun. Surv. & Tutorials*, vol. 23, no. 4, pp. 2630–2659, 2021.

[5] A. Brett, "Secrets of the deep: Defining privacy underwater," *Mo. L. Rev.*, vol. 84, p. 47, 2019.

[6] F. J. Lopez-Martinez, G. Gomez, and J. M. Garrido-Balsells, "Physical-layer security in free-space optical communications," *IEEE Photonics J*, vol. 7, no. 2, pp. 1–14, 2015.

[7] N. Skorin-Kapov, M. Furdek, S. Zsigmond, and L. Wosinska, "Physical-layer security in evolving optical networks," *IEEE Commun. Magazine*, vol. 54, no. 8, pp. 110–117, 2016.

[8] M. Soltani and Z. Rezki, "Optical wiretap channel with input-dependent Gaussian noise under peak-and average-intensity constraints," *IEEE Trans. Inf. Theory*, vol. 64, no. 10, pp. 6878–6893, 2018.

[9] J.-Y. Wang, C. Liu, J.-B. Wang, Y. Wu, M. Lin, and J. Cheng, "Physical-layer security for indoor visible light communications: Secrecy capacity analysis," *IEEE Trans. Commun.*, vol. 66, no. 12, pp. 6423–6436, 2018.

[10] R. Boluda-Ruiz, A. García-Zambrana, B. Castillo-Vázquez, and K. Qaraqe, "Secure communication for FSO links in the presence of eavesdropper with generic location and orientation," *Opt. Express*, vol. 27, no. 23, pp. 34 211–34 229, Nov 2019.

[11] R. Boluda-Ruiz, S. C. Tokgoz, A. García-Zambrana, and K. Qaraqe, "Enhancing secrecy capacity in FSO links via MISO systems through turbulence-induced fading channels with misalignment errors," *IEEE Photonics J.*, vol. 12, no. 4, pp. 1–14, 2020.

[12] "Autonomous underwater vehicle (AUV) market by type (shallow AUVs, medium AUVs, large AUVs), application (military & defense, oil & gas), shape, technology (navigation, imaging), payload type (cameras, sensors), region-global forecast to 2025," https://www.marketsandmarkets.com.

[13] A. D. Wyner, "The wire-tap channel," *Bell Labs Technical J.*, vol. 54, no. 8, pp. 1355–1387, 1975.

[14] E. Illi, F. El Bouanani, D. B. Da Costa, F. Ayoub, and U. S. Dias, "Dual-hop mixed RF-UOW communication system: A phy security analysis," *IEEE Access*, vol. 6, pp. 55 345–55 360, 2018.

[15] E. Illi, F. El Bouanani, D. B. da Costa, P. C. Sofotasios, F. Ayoub, K. Mezher, and S. Muhaidat, "Physical layer security of a dual-hop regenerative mixed RF/UOW system," *IEEE Trans. Sustain. Comput.*, vol. 6, no. 1, pp. 90–104, 2019.

[16] H. Lei, Y. Zhang, K.-H. Park, I. S. Ansari, G. Pan, and M.-S. Alouini, "Performance analysis of dual-hop RF-UWOC systems," *IEEE Photonics J.*, vol. 12, no. 2, pp. 1–15, 2020.

[17] A. Badrudduza, M. Ibrahim, S. R. Islam, M. S. Hossen, M. K. Kundu, I. S. Ansari, and H. Yu, "Security at the physical layer over GG fading and mEGG turbulence induced RF-UOWC mixed system," *IEEE Access*, vol. 9, pp. 18 123–18 136, 2021.

[18] Z. Zuo, Y. Wang, Y. Mao, X. Ruan, and Y. Guo, "Security of quantum communications in oceanic turbulence," *Phys Rev A*, vol. 104, no. 5, p. 052613, 2021.

[19] M. Kong, J. Wang, Y. Chen, T. Ali, R. Sarwar, Y. Qiu, S. Wang, J. Han, and J. Xu, "Security weaknesses of underwater wireless optical communication," *Opt. Express*, vol. 25, no. 18, pp. 21 509–21 518, 2017.

[20] Q. Hu, C. Gong, T. Lin, J. Luo, and Z. Xu, "Secrecy performance analysis for water-to-air visible light communication," *J. Lightwave Technol.*, vol. 40, no. 14, pp. 4607–4620, 2022.

[21] M. V. Jamali, P. Nabavi, and J. A. Salehi, "MIMO underwater visible light communications: Comprehensive channel study, performance analysis, and multiple-symbol detection," *IEEE Trans. Veh. Technol.*, vol. 67, no. 9, pp. 8223–8237, 2018.

[22] R. Boluda-Ruiz, P. Rico-Pinazo, B. Castillo-Vazquez, A. Garcia-Zambrana, and K. Qaraqe, "Impulse response modeling of underwater optical scattering channels for wireless communication," *IEEE Photonics J.*, vol. 12, no. 2, pp. 1–14, 2020.

[23] R. Boluda-Ruiz, A. García-Zambrana, B. Castillo-Vázquez, and S. Hranilovic, "Impact of angular pointing error on BER performance of underwater optical wireless links," *Opt. Express*, vol. 28, no. 23, pp. 34 606–34 622, 2020.

[24] A. S. Ghazy, S. Hranilovic, and M. A. A. Khalighi, "Angular MIMO for Underwater Wireless Optical Communications: Link Modelling and Tracking," *IEEE J. Ocean. Eng.*, vol. 46, no. 4, pp. 1391–1407, 2021.

[25] P. Salcedo-Serrano, R. Boluda-Ruiz, J. M. Garrido-Balsells, and A. García-Zambrana, "On the scattering-induced fading for optical wireless links through seawater: Statistical characterization and its applications," *Opt. Express*, vol. 29, no. 23, pp. 37 101–37 116, 2021.

[26] R. Boluda-Ruiz, P. Salcedo-Serrano, B. Castillo-Vázquez, A. García-Zambrana, and J. M. Garrido-Balsells, "Capacity of underwater optical wireless communication systems over salinity-induced oceanic turbulence channels with isi," *Opt. Express*, vol. 29, no. 15, pp. 23 142–23 158, 2021.

[27] V. I. Haltrin, "Chlorophyll-based model of seawater optical properties," *Applied Opt.*, vol. 38, no. 33, pp. 6826–6832, 1999.

[28] D. Stramski, A. Bricaud, and A. Morel, "Modeling the inherent optical properties of the ocean based on the detailed composition of the planktonic community," *Applied Opt.*, vol. 40, no. 18, pp. 2929–2945, 2001.

[29] F. Yang, J. Cheng, and T. Tsiftsis, "Free-space optical communication with nonzero boresight pointing errors," *IEEE Trans. Commun.*, vol. 62, no. 2, pp. 713–725, 2014.

[30] M. D. Soltani, E. Sarbazi, N. Bamiedakis, P. De Souza, H. Kazemi, J. M. Elmirghani, I. H. White, R. V. Penty, H. Haas, and M. Safari, "Safety analysis for laser-based optical wireless communications: A tutorial," *Proc. IEEE*, vol. 110, no. 8, pp. 1045–1072, 2022.

[31] C. D. Mobley, *Light and water: radiative transfer in natural waters*, Academic, 1994.

[32] H. M. Oubei, E. Zedini, R. T. ElAfandy, A. Kammoun, T. K. Ng, M.-S. Alouini, and B. S. Ooi, "Efficient weibull channel model for salinity induced turbulent underwater wireless optical communications," in *2017 Opto-Electronics and Communications Conference (OECC) and Photonics Global Conference (PGC)*, 2017, pp. 1–2.

[33] M. V. Jamali, A. Mirani, A. Parsay, B. Abolhassani, P. Nabavi, A. Chizari, P. Khorramshahi, S. Abdollahramezani, and J. A. Salehi, "Statistical studies of fading in underwater wireless optical channels in the presence of air bubble, temperature, and salinity random variations," *IEEE Trans. Commun.*, vol. 66, no. 10, pp. 4706–4723, 2018.

[34] R. Boluda-Ruiz, A. García-Zambrana, C. Castillo-Vázquez, and B. Castillo-Vázquez, "Novel approximation of misalignment fading modeled by Beckmann distribution on free-space optical links," *Opt. Express*, vol. 24, no. 20, pp. 22 635–22 649, 2016.

[35] I. S. Gradshteyn and I. M. Ryzhik, *Table of integrals, series and products*, 7th ed, Academic, 2007.

[36] V. Nikishov and V. Nikishov, "Spectrum of turbulent fluctuations of the sea-water refraction index," *Int. J. Fluid Mech. Res.*, vol. 27, no. 1, 2000.

[37] O. Korotkova, N. Farwell, and E. Shchepakina, "Light scintillation in oceanic turbulence," *Waves in Random and Complex Media*, vol. 22, no. 2, pp. 260–266, 2012.

[38] S. A. Thorpe, *The turbulent ocean*, Cambridge University Press, 2005.

[39] "The sonardyne site: Bluecomm underwater optical communications. Sonardyne International ltd." http://www.sonardyne.com/.

[40] "Thorlabs, inc." https://www.thorlabs.com/.

[41] R. Boluda-Ruiz, A. García-Zambrana, C. Castillo-Vázquez, B. Castillo-Vázquez, and S. Hranilovic, "Outage performance of exponentiated Weibull FSO links under generalized pointing errors," *J. Lightwave Technol.*, vol. 35, no. 9, pp. 1605–1613, 2017.

[42] Wolfram Research, Inc. The Wolfram functions site. [Online]. Available: http://functions.wolfram.com

[43] M. Bloch, J. Barros, M. R. Rodrigues, and S. W. McLaughlin, "Wireless information-theoretic security," *IEEE Trans. Inf. Theory*, vol. 54, no. 6, pp. 2515–2534, 2008.

[44] A. Lapidoth, S. Moser, and M. Wigger, "On the capacity of free-space optical intensity channels," *IEEE Trans. Inf. Theory*, vol. 55, no. 10, pp. 4449–4461, 2009.

[45] A. P. Prudnikov, Y. A. Brychkov, and O. I. Marichev, *Integrals and series Volume 3: More Special Functions*, Gordon and Breach Science Publishers, 1999, vol. 3.

[46] A. A. Kilbas, *H-transforms: Theory and Applications*, CRC Press, 2004.

[47] C. Castillo-Vazquez, R. Boluda-Ruiz, B. Castillo-Vazquez, and A. Garcia-Zambrana, "Outage performance of DF relay-assisted FSO communications using time-diversity," *IEEE Photonics Technol. Lett.*, vol. 27, no. 11, pp. 1149–1152, 2015.

[48] W.-S. Tsai, H.-H. Lu, H.-W. Wu, C.-W. Su, and Y.-C. Huang, "A 30 Gb/s PAM4 underwater wireless laser transmission system with optical beam reducer/expander," *Sci. Rep*, vol. 9, no. 1, pp. 1–8, 2019.

[49] "Edmund optics inc." https://www.edmundoptics.com/.

Rubén Boluda-Ruiz was born in Málaga, Spain, in 1986. He received the B.Sc. and M.Sc. degrees in Telecommunication Engineering (Electronics and Communications), and the Ph.D. degree in Electrical Engineering from the University of Málaga, Málaga, Spain, in 2012, 2014 and 2017, respectively.

From 2010 to 2013, he was a software engineer in the telecommunication industry. In 2016, he was a visiting researcher with the Department of Electrical and Computer Engineering, McMaster University, Hamilton, ON, Canada. From October 2017 to December 2019, he was a Post-Doctoral Research Associate with the Electrical and Computer Engineering Program, Texas A&M University at Qatar. From January 2020 to May 2021, he was a Post-Doctoral Researcher with the Communications Engineering Department, University of Málaga. Since May 2021, he is an Assistant Professor with the Communications Engineering Department, University of Málaga. He has authored/co-authored 50 journal and conference publications. His current research interests include theory and its application to design and performance analysis of terrestrial and underwater free-space optical (FSO) communication systems with current emphasis on channel modeling, multiple-input/multiple-output (MIMO) systems, physical layer security aspects, among others.

Dr. Boluda-Ruiz is an active reviewer for various IEEE and OSA top journals. He was a recipient of the best Ph.D. Thesis in Electrical Engineering (Extraordinary Doctorate Award) by the University of Málaga (2017-2018), the Best Ph.D. Thesis in Electrical Engineering in the XVI Night of Telecommunications by the Agencia Andaluza de Ingenieros de Telecomunicación (AAIT) in 2018, the TAMUQ Research Excellence Award 2018, and the Exmplary Reviewer Certificate of 2021 by IEEE Transactions on Communications.

Pedro Salcedo-Serrano was born in Granada, Spain, in 1997. He received the B.Sc and M.Sc degrees in Telecommunication Engineering (Acoustic and Communications), in 2019 and 2020, respectively, from the University of Málaga, Málaga, Spain. Since 2021, he is a Pre-Doctoral Researcher with the Communications Engineering Department, University of Málaga. His current research interests include information theory and its application to design and performance analysis of underwater optical wireless communication systems with current emphasis on underwater channel modeling.

Beatriz Castillo-Vázquez was born in Madrid, Spain, in 1971. She pursued her academic journey at the University of Málaga, where she obtained both her M.Sc. and Ph.D. degrees in Electrical Engineering in 1994 and 1999, respectively. She joined the Department of Communications Engineering at the University of Málaga in 1995, where she currently holds the position of Associate Professor. Her research interests primarily are related to the field of optical wireless communications, including free-space optics (FSO), underwater optical wireless communications (UOWC), channel modeling, relay/multihop communications and physical layer secrecy issues.

Antonio García-Zambrana was born in Málaga, Spain, in 1970. He pursued his academic journey at the University of Málaga, where he obtained both his M.Sc. and Ph.D. degrees in Electrical Engineering in 1994 and 1998, respectively. Following his education, he joined the Department of Communications Engineering at the University of Málaga in 1994, and he currently holds the position of Full Professor there. Prof. A. Garcia-Zambrana has made significant contributions to the field of optical wireless communications. His research interests primarily revolve around this area, encompassing various aspects such as free-space optics, underwater optical wireless communications, channel modeling, relay/multihop communications and physical layer secrecy issues.

José María Garrido-Balselss was born in Granada, Spain, in 1974. He received the M.S. degree (1999) and the Ph.D. degree (2008) in Telecommunications Engineering from the University of Málaga, Spain.

He worked for 3 years as a consultant and technical manager for several telecommunications companies. In 2001 he joined the Communications Engineering Department of the University of Malaga as a full-time Assistant Professor (LRU), where currently, he is Associate Professor. Since 2001, he is with the TIC-102 research group of the Regional Government of Andalusia and since 2020 he is also with the TELMA Research Institute in the University of Málaga. He has authored and co-authored 70 journal and conference publications, participating actively as principal investigator in research projects and contracts with national and international companies. His research interests include topics as wireless optical communications, including indoor, visual light communications (VLC) and outdoor optical communications systems through turbulent and dispersive media such atmospheric or underwater. He is also interested in topics related to adaptive optics applications including machine learning control algorithms, structured light and OAM vortex beams or channel coding schemes, among others.